CVEL

THE CLEMSON UNIVERSITY VEHICULAR ELECTRONICS LABORATORY

TECHNICAL REPORT: CVEL-10-017.01

Investigation of the Imbalance Difference Model and its Application to Various Circuit Board and Cable Geometries

Hocheol Kwak and Dr. Todd Hubing
Clemson University

May 21. 2011

Table of Contents

Abstract

The imbalance difference model introduced by Watanabe is a method for modeling how differential-mode signal currents are converted to common-mode noise currents. A parameter called the *current division factor* or *imbalance factor* uniquely defines the degree of imbalance of a transmission line. The imbalance difference model shows that changes in the imbalance are responsible for differential-mode to common-mode conversion. This paper explores various cable geometries to determine how well common-mode currents obtained using the imbalance difference model compare to full-wave calculations. It also demonstrates how the imbalance difference model can be used to model the differential-mode to common-mode conversion in cables with more than two conductors.

1. Introduction

Determining the distribution of signal and noise currents in circuit boards or electronic systems is an important step in analyzing sources of electromagnetic interference. In a two-conductor transmission line, currents that flow in one direction on one conductor and in the opposite direction on the other conductor (differential-mode) are not likely to be a significant source of radiated emissions. On the other hand, currents that flow in the same direction on both conductors (common-mode) are often a primary source of radiated emissions [1], [2]. While differential-mode currents are generally intentional, common-mode currents are often the result of unintentional differential-to-common-mode conversion resulting from electrical imbalance.

Several models have been introduced to describe differential-mode to common-mode conversion. Hockanson [3], [4] introduced current-driven and voltage-driven source models to describe how differential-mode signals on circuit boards induce common-mode currents on attached wires.

Shim [5] developed an equivalent model for estimating the radiated emissions from a printed circuit board with attached cables driven by a signal voltage on a trace. This model employed an equivalent common-mode voltage source located at the junction between the PCB ground structure and the attached wire. The magnitude of the common-mode voltage was proportional to the ratio of the self-capacitance of the trace to the return plane of PCB structure (effectively a measure of imbalance).

Watanabe et al. [6]-[9] introduced the concept of an *imbalance difference factor* to quantify the electrical imbalance of various transmission line configurations. He showed that imbalance is not responsible for the conversion of differential-mode currents to common-mode currents. Instead, it is changes in imbalance that facilitate this conversion. Using various printed circuit board structures as examples, he showed that it is possible to calculate the common-mode currents by replacing the differential-mode source with equivalent common-mode sources at points where changes in the imbalance occur. This imbalance difference modeling technique can greatly simplify the analysis of radiated emissions due to common-mode currents. Su [10] showed that the imbalance difference model could be used in place of the voltage-driven and current-driven models for calculating radiated emissions from cables attached to printed circuit boards.

In this paper, the imbalance difference theory is extended to apply to structures with more than one differential-mode current. The procedure is demonstrated using a three-phase power system example, but can be generally extended to apply to multi-wire cable geometries in other applications.

2. The Imbalance Difference Model

A two-wire transmission line circuit with a voltage source (V_s), source impedances (Z_{S1}, Z_{S2}, Z_{SG1}, and Z_{SG2}), load impedances (Z_{L1}, Z_{L2}, and Z_{LG}), and cable impedances ($Z_{CableG1}$ and $Z_{CableG2}$) is shown in Fig. 1. The currents, I_1 and I_2 flow on each transmission line conductor. These currents can be

decomposed into differential-mode and common-mode components. If we assume that the two conductors are perfectly balanced ($Z_{S1} = Z_{S2}$, $Z_{SG1} = Z_{SG2}$, $Z_{L1} = Z_{L2}$, $Z_{CableG1} = Z_{CableG2}$), the currents, I_1 and I_2, have equal magnitude but opposite direction and the common-mode component is zero. If one side of the circuit has a different impedance to ground than the other side, then the circuit is not perfectly balanced. According to the imbalance difference theory, any change in the imbalance in a circuit results in the conversion of differential-mode currents into common-mode current. We can define a current division factor (or *imbalance factor*), h, that describes how much of the common-mode current flows on each conductor as,

$$\begin{bmatrix} I_1 \\ I_2 \end{bmatrix} = \begin{bmatrix} h & 1 \\ 1-h & -1 \end{bmatrix} \begin{bmatrix} I_{CM} \\ I_{DM} \end{bmatrix} \tag{1}$$

where $0 \leq h \leq 1$, and perfect balance is achieved when $h = 0.5$.

In an unbalanced circuit, the common-mode current is not divided equally between the two conductors. Rearranging (1), the currents, I_1 and I_2 can be decomposed into common-mode and differential-mode components,

$$\begin{bmatrix} I_{DM} \\ I_{CM} \end{bmatrix} = \begin{bmatrix} 1-h & -h \\ 1 & 1 \end{bmatrix} \begin{bmatrix} I_1 \\ I_2 \end{bmatrix} \tag{2}$$

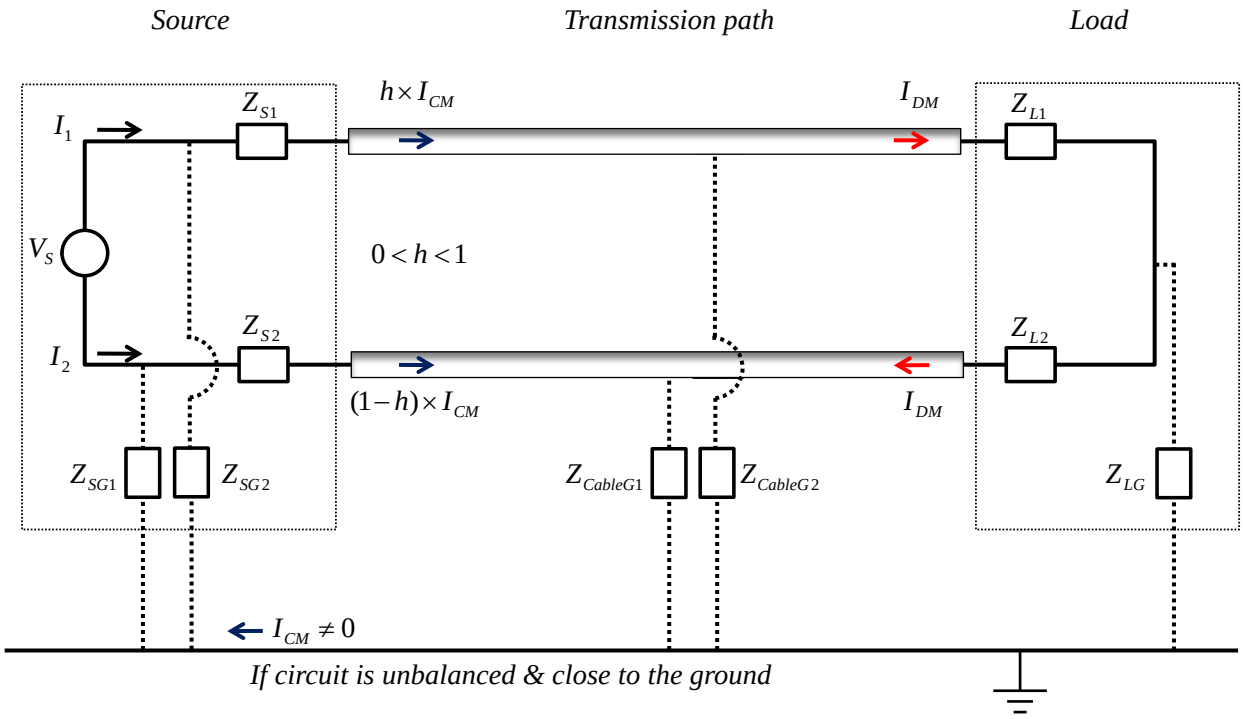

Fig. 1. Current flow decomposition of two-transmission line circuit.

The imbalance difference method is a method for modeling how differential-mode signal currents are converted to common-mode noise currents. The imbalance factor can be determined from the capacitances of each conductor to ground.

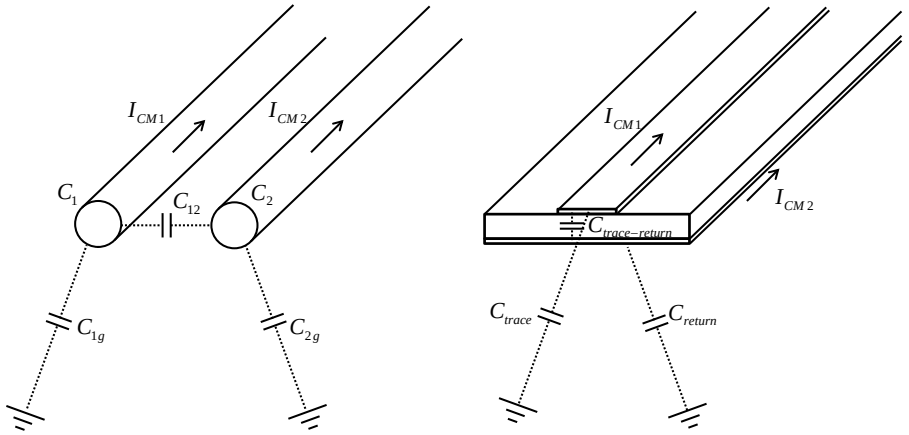

(*a*) Two-wire transmission line (*b*) Microstrip structure

Fig. 2. Stray capacitance for two transmission geometries.

For example, for the transmission line geometries in Fig. 2, the imbalance factor, *h*, can be described in terms of the per-unit-length capacitances [7],

$$h = \frac{C_{1g}}{C_{1g} + C_{2g}}. \tag{3}$$

For TEM propagation, this can be shown to be equal to the static charge distribution that is obtained when both conductors have the same voltage relative to ground,

$$h = \frac{Q_1}{Q_1 + Q_2}. \tag{4}$$

Note that "ground" may be a nearby metal structure (e.g. a ground plane or chassis), or it may represent a point far away (e.g. at infinity). When the ground is nearby, the common-mode currents are generally the currents that return to the source on the nearby ground conductor. When the ground is far away, the common-mode currents are "antenna mode" currents that return to the source as displacement current. The imbalance difference method applies equally well in either situation.

In order to evaluate the common-mode current distribution on an EMI antenna structure, the imbalance difference model postulates that the common-mode currents on a transmission line can be precisely determined by removing all differential-mode sources from a circuit and placing equivalent common-mode sources at all points where a change in the imbalance occurred. The amplitude of these equivalent voltage sources is given by

$$V_{CM} = \Delta h \times V_{DM}(x) \tag{5}$$

where Δh is the changed in the imbalance factor and V_{DM} is differential-mode voltage at the point, x, where the change in imbalance occurs.

3. Modeling of Common-Mode Current Distributions

3.1 Wire model with voltage and current driven source

A two-wire transmission line with one of the wires extended at both ends is illustrated in Fig. 3 [3]. The electrical length of the entire circuit is short in terms of the free-space wavelength (10 m at 30 MHz). The wire radius is 0.8 mm. The vertical wires have a length of 10 mm. V_S = 1 volt at 30 MHz. R_S = 50 Ω. The length of each wire attached to the loop circuit is 30 cm.

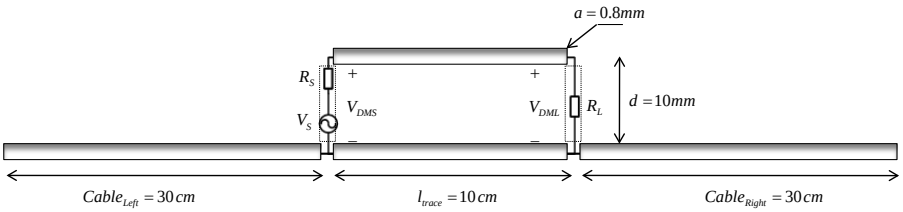

(a) Original circuit

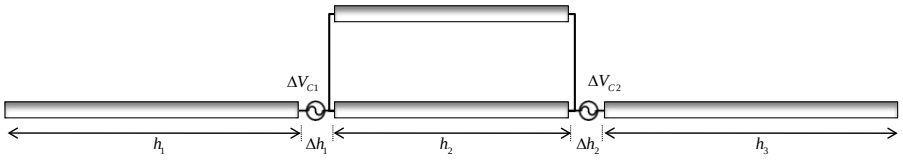

(b) Imbalance difference model

Fig. 3. A wire circuit geometry and its equivalent imbalance difference model.

The common-mode current induced in this structure including the two wires on each side of the circuit was computed using a full-wave electromagnetic modeling code [14]. Simulations were run with three load impedances: an open circuit, a short circuit and a 50-Ω load.

The magnitude of the common-mode current for the open circuit ($R_L = \infty$) case is indicated by the solid black curve in Fig. 4. Note that the common-mode current peaks at either end of the transmission line structure and is zero at the center.

The solid blue curve shows the magnitude of the common-mode current for the short circuit case (R_L = 0). In this case, the common-mode current peaks at the source end of the transmission line. The solid red curve shows the common-mode current when R_L = 50 Ω, which is a superposition of the currents for the short- and open-circuit cases.

According to the imbalance difference model, the geometry in Fig. 3(b) is equivalent to the geometry in Fig. 3(a) in terms of the common mode currents produced. The amplitude of the equivalent voltage sources is determined by (5). At the source end, Δh = 0.5 as the geometry transitions from perfectly unbalanced (h = 1.0, since there is only one conductor) to perfectly balanced (h = 0.5, since the two conductors are identical). At the load end, Δh = -0.5 as the geometry transitions from perfectly balanced to perfectly unbalanced.

Table I shows the common-mode excitation voltages, ΔV_{C1} and ΔV_{C2}, for each load impedance when the differential-mode source voltage is 1 V. The differential-mode voltage, V_{DMS} at the source location is given by,

$$V_{DMS} = V_S \frac{Z_{in}}{R_S + Z_{in}}, \tag{6}$$

where Z_{in} is the input impedance of the transmission line.

Table I. Voltages for the circuits in Fig. 3.

Source/Load impedance	V_{DMS}	ΔV_{C1}	V_{DML}	ΔV_{C2}
R_S = 50Ω R_L=50Ω	0.53∠ 9.8	0.26∠ 9.8	0.49∠ -11.1	0.25∠ 168.9
R_S = 50Ω R_L= open	1∠ 0	0.5∠ 0	1∠ 0	0.5∠ 180
R_S = 50Ω R_L= short	0.36∠ 69.2	0.18∠ 69.2	0	0

Full-wave common-mode current calculations for the structure in Fig. 3(b) are indicated by the dotted lines in Fig. 4. These results are labeled IDM (for Imbalance Difference Model) and are virtually identical to the results obtained by the full-wave analysis of the original configuration in Fig. 3(a).

The imbalance difference model for the open-circuit case consists of two equal and opposite sources located at each end of the transmission line structure. The symmetric nature of this model makes it clear that the common-mode currents must be zero at the center.

The imbalance difference model for the short-circuit case has only one non-zero equivalent source located at the source end of the transmission line. It is clear from the model that the common-mode currents must peak at the source end of the transmission line and decrease to zero at the end of each wire. This simple example demonstrates both the accuracy of the imbalance difference model, and its ability to provide an intuitive understanding of how and where differential-mode currents are converted to common-mode currents.

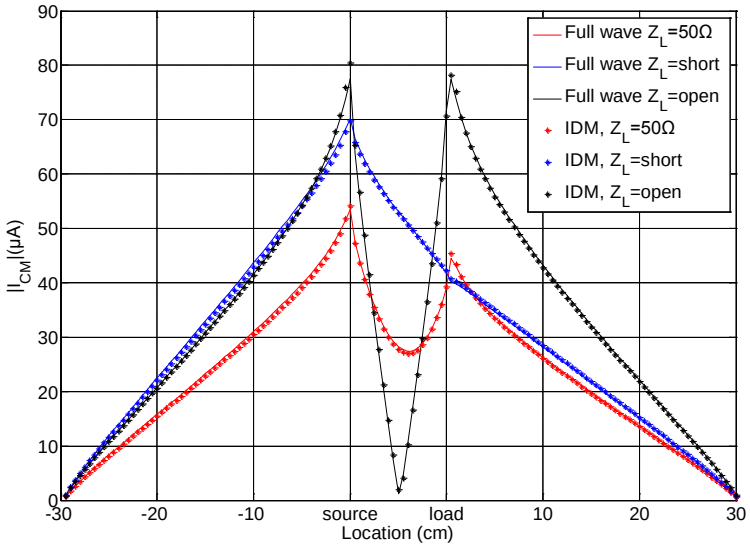

Fig. 4. Common-mode current distribution at 30 MHz.

3.2 Cable structure attached to a PCB

Fig. 5 shows a simple printed circuit board configuration and its equivalent imbalance difference model. The return plane dimensions are 10 cm by 4 cm. A 1-mm wide trace is located 3 mm above the plane (this dimension is exaggerated in the figure for clarity), and a 100-cm wire is attached to the return plane of the board and oriented horizontally. A 1-volt source in series with a 50-Ω source impedance is located between trace and the return plane at the left side of the board. The other side of the trace is terminated with a 50-Ω resistor. The board is located far away from any other conductors.

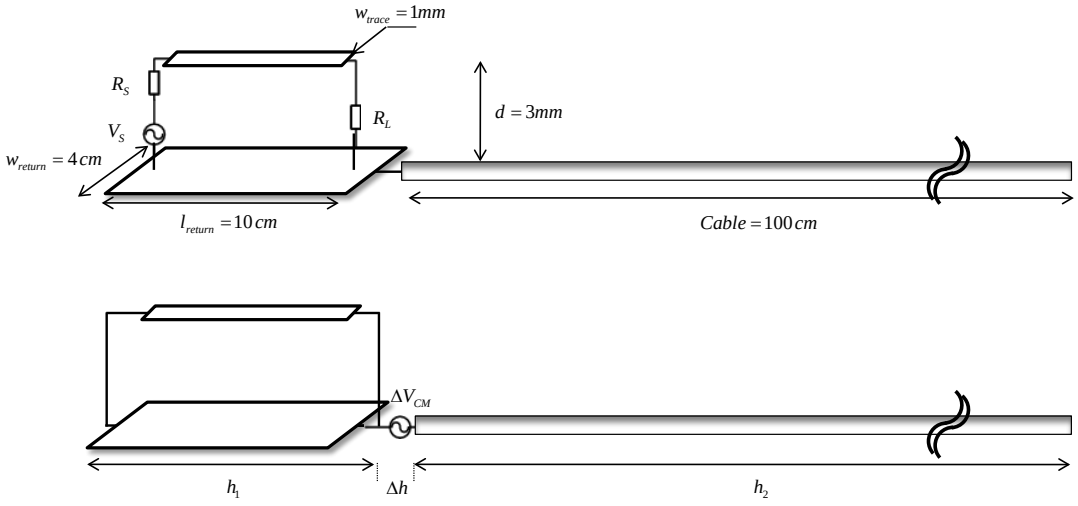

Fig. 5. PCB model with attached wire (top) and its imbalance difference model (bottom).

The imbalance factor, *h*, for the imbalance difference model is obtained from the ratio of the stray capacitance of the trace to the stray capacitance of the return plane of the board as described in (3), where the "ground" is at infinity because we are interested in the antenna-mode currents induced on the wire. The stray capacitance of the trace and the return plane of the board can be computed by two methods: an approximate closed-form solution or a 2D-FEM simulation.

A closed-form solution for the stray capacitance of a trace in a microstrip structure is provided in [11],

$$C_t \approx \frac{6.189}{\pi}\frac{d}{W}\frac{C_{DM} l_t}{\ln\left[1+3.845\left(\frac{L}{W}\right)\right]}, \tag{7}$$

where L and W are the length and width of the board, l_t is length of the trace, d is the distance between the trace and the return plane of the board, and C_{DM} is the capacitance of the trace over an infinitely wide return plane. The stray capacitance of the board is approximately [5],

$$C_{board} \approx 8\varepsilon_0\sqrt{\frac{Board\ \ Area}{\pi}}\,. \tag{8}$$

Table II shows the capacitances and imbalance factors calculated using the closed form equations and also those calculated using the 2D FEM simulation [15].

Table II. Comparison of imbalance factor calculations

	C_{Board}	C_{trace}	h
Closed form	2.53	0.11	0.042
FEM	2.57	0.08	0.048

Fig. 6 shows the magnitude of the common-mode current induced on the attached cable as determined by a full-wave model of the entire configuration, an IDM model based on the imbalance factors computed by the 2D FEM code, and an IDM model based on the closed form calculations of the imbalance factor. The magnitude of the common-mode current is highest at the junction between the printed circuit board and the wire. There is excellent agreement between the full-wave model and the imbalance difference model (IDM) employing the 2D FEM. Both models calculate a current of approximately 12 μA at the board-cable junction. The IDM results obtained using the closed-form imbalance factor estimates a slightly lower magnitude, ~10 μA.

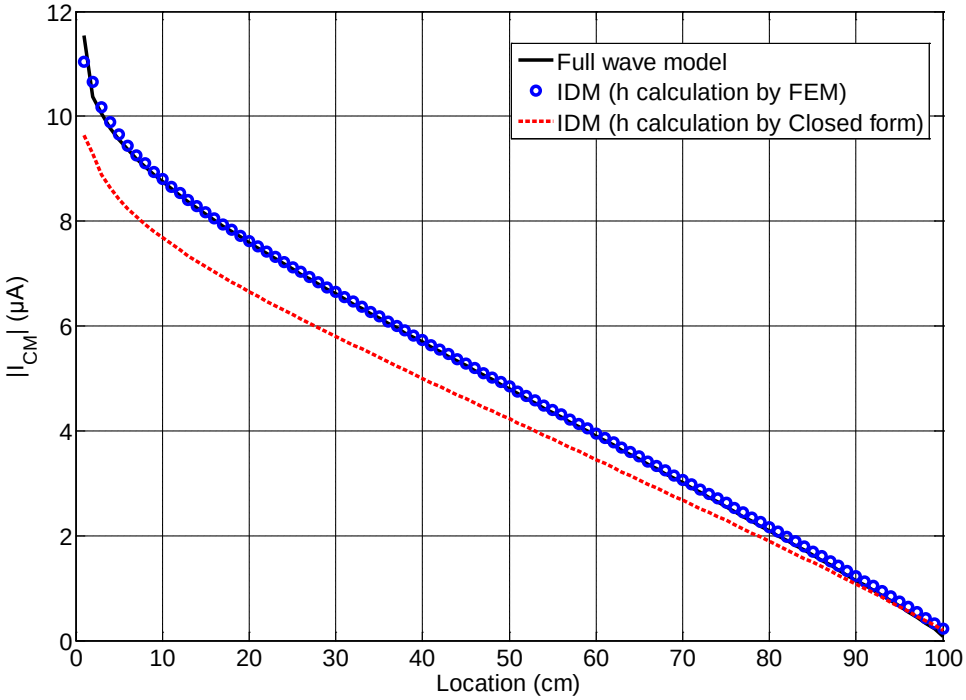

Fig. 6. Common-mode current distribution at 30 MHz.

3.3 Long wire model with imbalance

Fig. 7 shows a 2-wire transmission line structure where the radius of one wire changes in the middle represented as the sum of two alternative structures: one that is perfectly balanced and carries only differential-mode currents, and one that is the equivalent imbalance difference model and carries only common-mode current. From the imbalance difference model, we know that a change in the balance occurring at the center of an electrically short transmission line will result in a common-mode current distribution that peaks in the center and goes to zero at both ends.

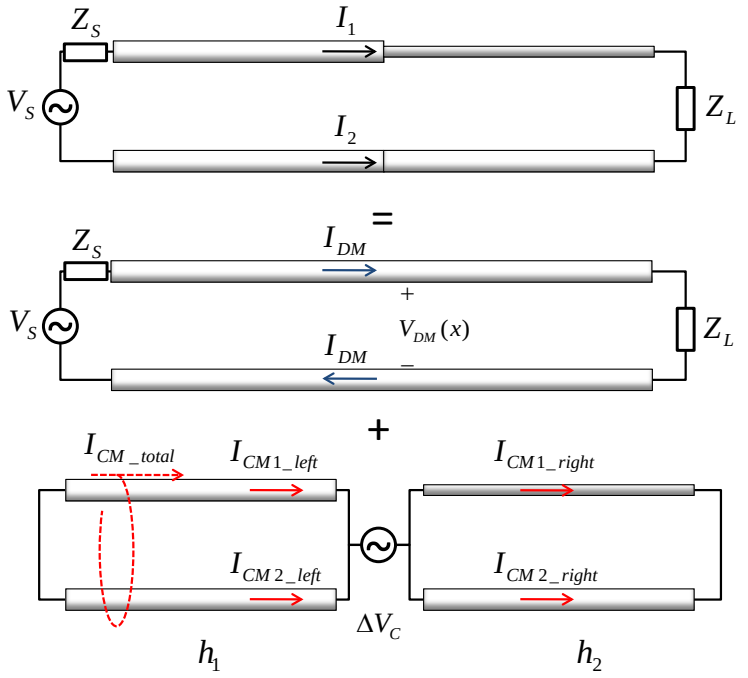

Fig. 7. Long wire circuit (top) and its decomposition (transmission line and antenna mode).

Fig. 8 shows the dimensions of the wires in the configuration modeled. The right half of the transmission line has different wire radii, *a* and *b*. The characteristic impedance of this part of the transmission line can be calculated as [12],

$$Z_{01} = 60\cosh^{-1}\left[\frac{1}{2}\left(\frac{d^2}{ab} - \frac{a}{b} - \frac{b}{a}\right)\right]. \tag{9}$$

The wires on the left half of the transmission line have the same radius, *a*. The characteristic impedance of this transmission line is given by,

$$Z_{02} = 120\cosh^{-1}\left(\frac{d}{2a}\right) \tag{10}$$

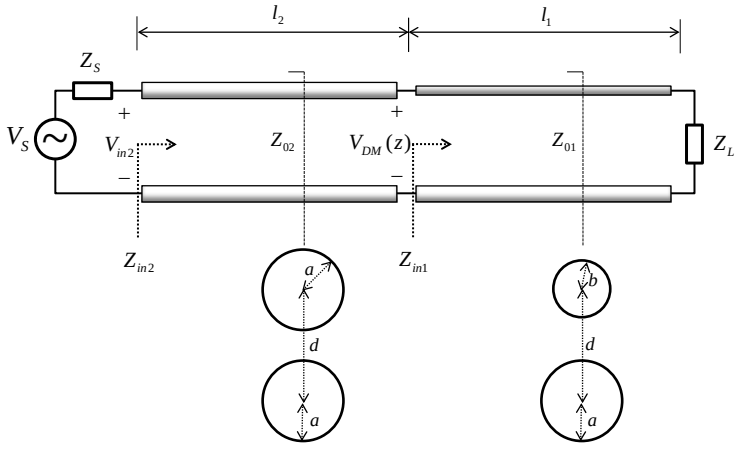

Fig. 8. Cross-sectional view of Fig. 7 transmission line structure.

At the source location, the input voltage is,

$$V_{in2} = V_S \frac{Z_{in2}}{Z_S + Z_{in2}}, \tag{11}$$

where $Z_{in2} = Z_{02} \dfrac{Z_{in1} + jZ_{02}\tan(\beta l)}{Z_{02} + jZ_{in1}\tan(\beta l)}$ and $Z_{in1} = Z_{01} \dfrac{Z_L + jZ_{01}\tan(\beta l)}{Z_{01} + jZ_L\tan(\beta l)}$.

At the location of the discontinuity, the differential-mode voltage is

$$V_{DM}(l_1) = V_S \frac{Z_{in2}}{Z_S + Z_{in2}} \left(\frac{1+\rho_L}{e^{j\beta l_2} + \rho_L e^{-j\beta l_2}} \right), \tag{12}$$

where $\rho_L = \dfrac{Z_{in1} - Z_{02}}{Z_{in1} + Z_{02}}$.

The amplitude of the equivalent common-mode voltage source can be calculated from (5) using the differential-mode voltage determined from (12).

Two parallel wires having radius a_1 and a_2, respectively, and a separation distance, d, can be modeled by one wire having an equivalent radius a_e where [13],

$$\ln(a_e) \cong \frac{1}{(S_1 + S_2)^2} \times \left[S_1^2 \ln a_1 + S_2^2 \ln a_2 + 2S_1 S_2 \ln d \right] \tag{13}$$

as illustrated in Fig. 9. Typically, when applying the imbalance difference model, the equivalent source drives all the conductors on one side of the imbalance discontinuity relative to all conductors on the other side of the discontinuity as illustrated by the configuration labeled IDM in Fig. 9. In many cases, it is possible to represent the conductors on each side of the discontinuity with a single conductor as illustrated by the configuration labeled “Equivalent Dipole Antenna” in Fig. 9.

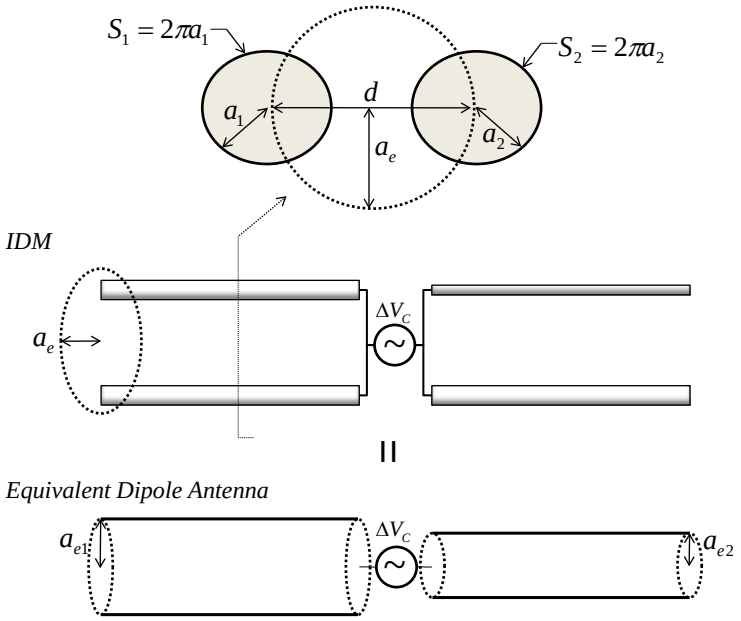

Fig. 9. Equivalent geometric conversion from two conductors to one [16].

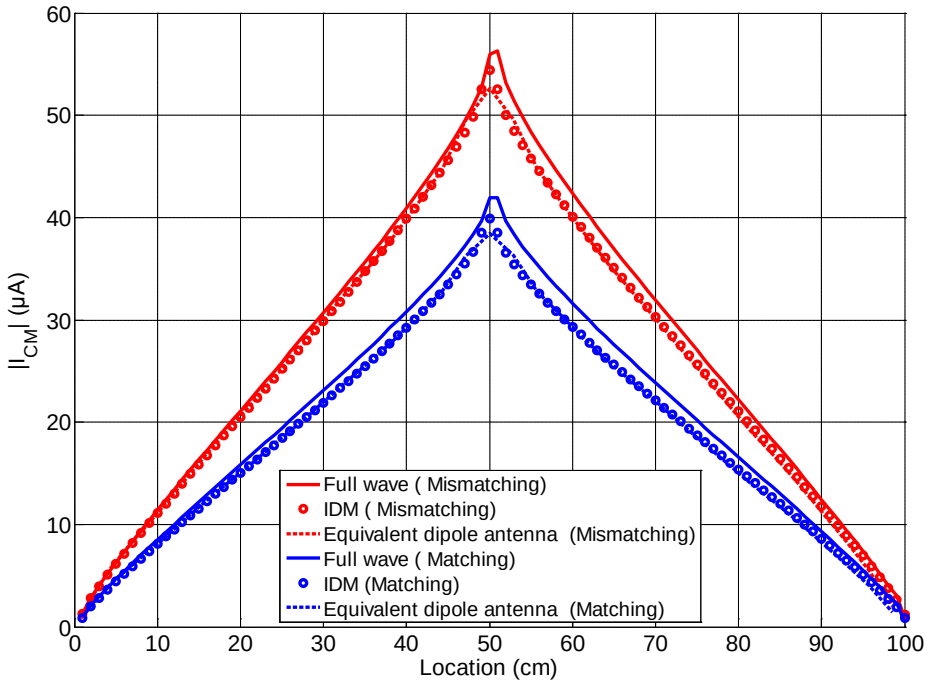

Fig. 10. Common-mode current on the structure in Fig. 8 (matched and unmatched).

Fig. 10 shows the common-mode currents obtained from a full-wave model of the whole configuration, an IDM model and an equivalent dipole antenna driven by an IDM equivalent source. The excitation frequency is 30 MHz and the wire is 100 cm long (50 cm per section). Each wire on the left half of the transmission line has same radius, 2.5 mm; however on the right half of the transmission line the radius of one of the wires increases to 5.0 mm. The center-to-center spacing of the wires is 7.5 mm. The red curves were obtained with source and load impedances that were mismatched to the characteristic impedance of transmission line. In this case, the source impedance was 50 Ω and the load impedance was 100 Ω. The characteristic impedances of each half of the transmission line, Z_{01} and Z_{02} are 164.2 and 115.5 Ω, respectively. The blue curves were obtained with source and load impedances that were matched to the characteristic impedance of the transmission line. The source impedance was Z_{02} = 115.5 Ω and the load impedance was $Z_L = Z_{01}$ = 164.2 Ω. The magnitude of common-mode current was lower when impedances were matched because the differential-mode voltage at the point of the imbalance change was lower.

4. Multi-wire Configurations

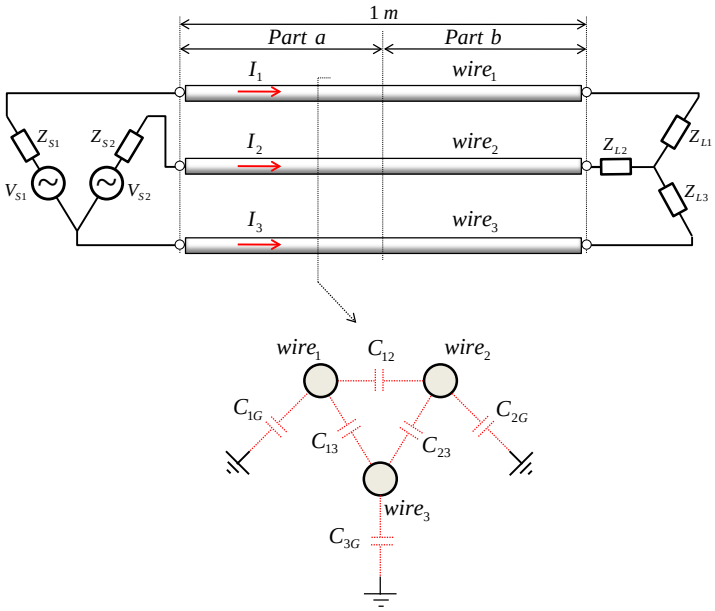

Fig. 11. A three-phase circuit with two differential-mode sources and y-connected loads.

Previously published work has not addressed the problem of multi-wire configurations where there are multiple differential-modes. For example, in a three-phase transmission line, two independent differential mode currents can be defined. The three-phase system illustrated in Fig. 11 has two independent differential-mode voltage sources, V_{S1} and V_{S2}. The system is terminated by three load impedances, Z_{L1}, Z_{L2}, and Z_{L3}, connected in a "Y" configuration. A change in the radius of one or more wires in the middle of the transmission line creates an imbalance difference that causes differential-mode to common-mode conversion.

Since there is more than one differential-mode signal that may be converted to common-mode current, more than one equivalent source is required to model this conversion. The total common-mode current in a three-phase system is the sum of the currents flowing on each wire,

$$I_{CM} = I_1 + I_2 + I_3 . \tag{14}$$

Each of the differential-mode signals encountering a change in imbalance contributes to this common-mode current. In Fig. 11, we've chosen conductor 3 as the reference for our two independent differential-mode signals, so we denote the voltage between lines 1 and 3 with the subscript "1" and the voltage between lines 2 and 3 with the subscript "2". Quantities on the left- and right-hand sides of the imbalance discontinuity are denoted by the subscripts "a" and "b", respectively. Using this notation, we can define four imbalance factors corresponding to the imbalance associated with the two differential-mode signals on the left- and right-hand sides of the transmission line;

$$h_{1a} = \frac{C_{1Ga}}{C_{1Ga} + C_{2Ga} + C_{3Ga}}, \; h_{1b} = \frac{C_{1Gb}}{C_{1Gb} + C_{2Gb} + C_{3Gb}} \tag{15a}$$

$$h_{2a} = \frac{C_{2Gb}}{C_{1Gb} + C_{2Gb} + C_{3Gb}}, \; h_{2b} = \frac{C_{2Gb}}{C_{1Gb} + C_{2Gb} + C_{3Gb}} \; . \tag{15b}$$

where, C_{iGn} is the self-capacitance (capacitance to ground at infinity) of the ith conductor on side n.

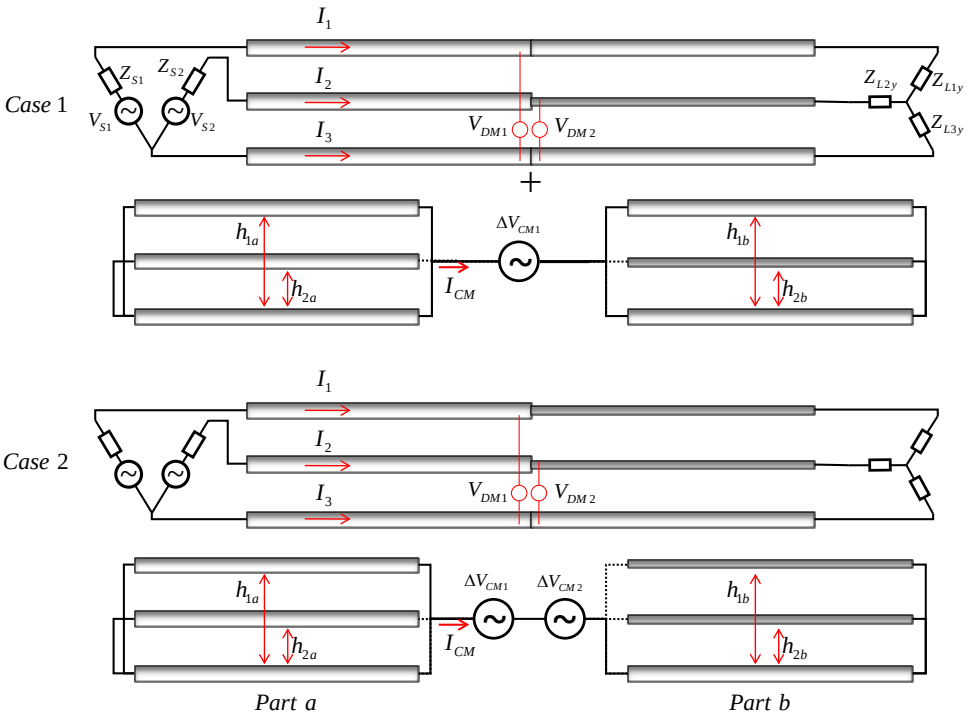

Fig. 12. Imbalance difference models for 2 three-phase circuits.

The equivalent common-mode voltages at discontinuity points were determined by the following equations based on the superposition theorem,

$$V_{CM1} = \Delta h_1 V_{DM1} + \Delta h_2 V_{DM2} \tag{16}$$

$$V_{CM2} = \Delta h_1 V_{DM1} + \Delta h_2 V_{DM2} \tag{17}$$

where V_{DMi} is the ith independent differential-mode voltage at the point of the imbalance change and $\Delta h_1 = h_{1b} - h_{1a}$, $\Delta h_2 = h_{2b} - h_{2a}$.

The total common-mode excitation due to imbalance difference is the sum of the common-mode excitations,

$$V_{CM} = V_{CM1} + V_{CM2}\,. \tag{18}$$

In general, for multi-wire transmission lines, the equation for the equivalent common-mode source voltage is,

$$V_{CM} = \sum_i \Delta h_i V_{DMi} \tag{19}$$

where V_{DMi} is the ith independent differential-mode voltage at the point of the imbalance change, and Δh_i is the change in the imbalance experienced by that component of the signal.

Multiple common-mode excitations due to the imbalance in a circuit with multiple wires can be described as the sum of each common-mode excitation as illustrated in Fig. 12. Case 1 is an example where one wire's diameter changes in the middle of the cable. In Case 2, two wires exhibit a change in diameter.

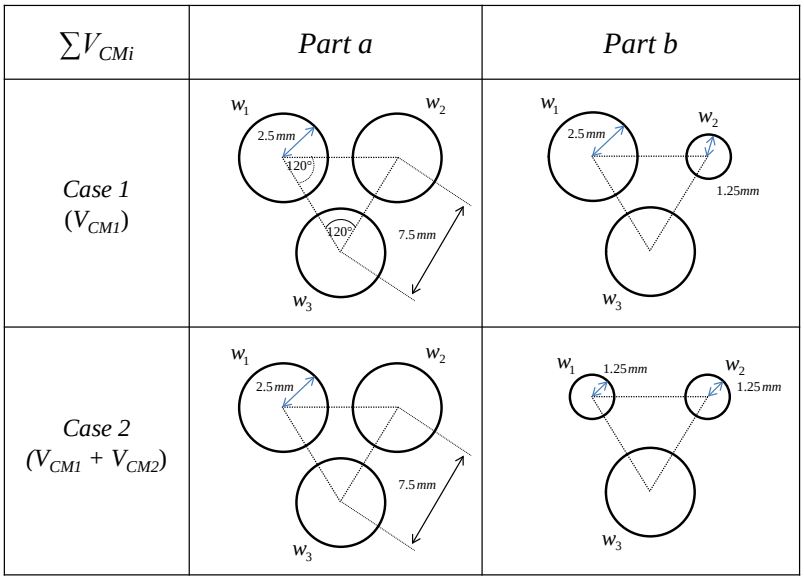

Fig. 13. Detailed geometry expression for multiple common-mode excitations.

Fig. 13 shows the cross-sections of the wire geometries in Fig. 12. The circuits evaluated have two differential-mode voltage sources with 1-V amplitudes and 50-Ω source impedances connected to three y-connected 50-Ω resistors. The transmission line between the source and load is 1 meter long. As illustrated in Fig. 13, two cases were modeled. In Case 1, there is one discontinuity resulting in one equivalent common-mode source. In Case 2, there are two discontinuities and two equivalent common-mode sources.

Fig. 14 compares the common-mode currents obtained by full-wave simulation on the original structure (solid curve) to the common-mode currents on the IDM structure (dotted curves) for each case. The blue curves are the results for Case 1 and the black curves are the results for Case 2. In each case, there is excellent agreement between the original circuit results and the imbalance difference model results

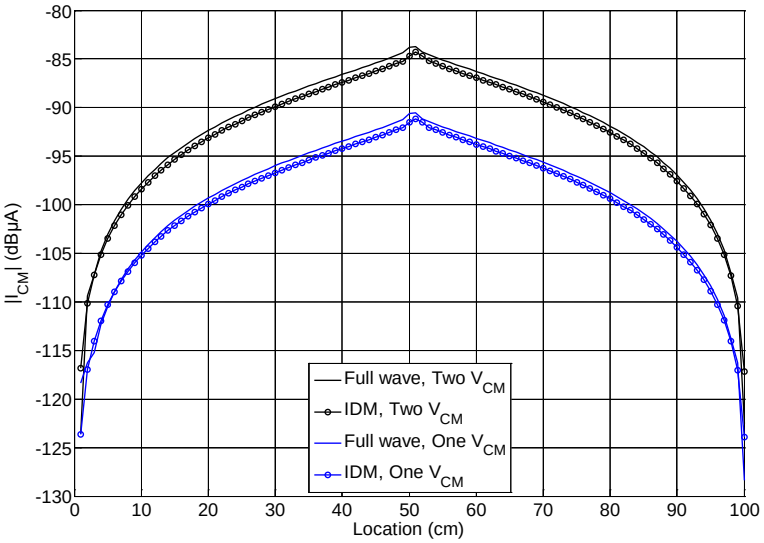

Fig. 14. Two differential-mode sources and single imbalance wire.

5. Conclusion

The imbalance difference model describes how changes in the imbalance of a circuit result in the conversion of differential-mode signals to common-mode noise. A parameter called the *current division factor* or *imbalance factor* uniquely defines the degree of imbalance experienced by a differential-mode signal at any location as it moves through a circuit. Various cable and printed circuit board geometries have been evaluated to illustrate how calculations of the common-mode currents on structures can be simplified and better understood using the imbalance difference model. A technique for applying the imbalance difference model to multi-wire structures with more than one differential-mode signal was also introduced. This technique superimposes the equivalent common-mode voltage sources for each independent differential-mode signal that encounters a change in electrical imbalance. In each case evaluated by the authors, the common-mode currents on the simplified structure obtained using the imbalance difference model were virtually identical to the common-mode currents in the original configuration.

References

[1] C. R. Paul, "A comparison of the contributions of common-mode and differential-mode currents in radiated emissions," *IEEE Trans. Electromag. Compat.*, vol. 31, no. 2, pp. 189-193, May 1989.

[2] K. B. Hardin and C. R. Paul, "Decomposition of radiating structures using the ideal structure extraction methods (ISEM)," *IEEE Trans. Electromag. Compat.*, vol. 35, no. 2, pp. 264-273, May 1993.

[3] D. M. Hockanson, J. L. Drewniak, T. H. Hubing and T. Van Doren, "Investigation of fundamental EMI source mechanisms driving common-mode radiation from printed circuit boards with attached cables," *IEEE Trans. Electromag. Compat.,* vol. 38, no. 4, pp. 557-566, Nov. 1996.

[4] D. M. Hockanson, J. L. Drewniak, T. H. Hubing and T. Van Doren, "Quantifying EMI resulting from finite-impedance reference planes," *IEEE Trans. Electromag. Compat.,* vol. 39, no. 4, pp. 286-297, Nov. 1997.

[5] Hwan Woo Shim and Todd H. Hubing, "Model for estimating radiated emissions from a printed circuit board with attached cables due to voltage-driven sources," *IEEE Trans. Electromag. Compat.*, vol. 47, no. 4, pp. 899-907, Nov. 2005.

[6] Tetsushi Watanabe, Osami Wada, Takuya Miyashita, and Ryuji Koga, "Common-mode-current generation caused by difference of unbalance of transmission lines on a printed circuit board with narrow ground pattern," *IEICE Trans. Commun*., vol. E83-B, no. 3, pp. 593-599, March 2000.

[7] Tetsushi Watanabe, Hiroshi Fujihara, Osami Wada and Ryuji Koga, "A prediction method of common-mode excitation on a printed circuit board having a signal trace near the ground edge," *IEICE Trans. Commun.,* vol. E87-B, no. 8, pp. 2327-2334, Aug. 2004.

[8] Tohlu Matsushima, Tetsushi Watanabe, Yoshitaka Toyota, Ryuji Koga and Osami Wada, "Increase of common-mode radiation due to guard trace voltage and determination of effective via-location," *IEICE Trans. Commun.*, vol. E92-B, no. 6, pp. 1929-1936, Jun. 2009.

[9] Tohlu Matsushima, Tetsushi Watanabe, Yoshitaka Toyota, Ryuji Koga and Osami Wada, "Evaluation of EMI reduction effect of guard traces based on imbalance difference method," *IEICE Trans. Commun.*, vol. E92-B, no. 6, pp. 2193-2200, Jun. 2009.

[10] Changyi Su and Todd Hubing, "Imbalance difference model for common-mode radiation from printed circuit board," *IEEE Trans. Electromag. Compat.*, vol. 53, no. 1, Feb. 2011, pp. 150-156.

[11] Hwan W. Shim and Todd H. Hubing, “Derivation of a closed form approximate expression for the self-capacitance of a printed circuit board trace,” *IEEE Trans. Electromag. Compat.*, vol. 47, no. 4, pp. 1004-1008, Nov. 2005.

[12] Kenneth L. Kaiser, *Electromagnetic Compatibility Handbook*, CRC Press, 2004.

[13] Constantine A. Balanis, *Antenna Theory, 3rd Edition*, John Wiley & Sons, Inc., 2005.

[14] FEKO User’s Manual, Suite 5.5, Electromagnetic Software and Systems, Stellenbosch, South Africa, Jul. 2009.

[15] Q2D/Q3D Extractor User’s Manual, Ver. 9.0, ANSYS, Sep. 2010.